

Probing electron trapping by current collapse in GaN/AlGaN FETs utilizing quantum transport characteristics

Takaya Abe,^{1,2} Motoya Shinozaki,^{3,*} Kazuma Matsumura,^{1,2} Takumi Aizawa,^{1,2} Takeshi Kumasaka,¹ Norikazu Ito,⁴ Taketoshi Tanaka,⁴ Ken Nakahara,⁴ and Tomohiro Otsuka^{3,1,2,5,6,†}

¹*Research Institute of Electrical Communication, Tohoku University,*

2-1-1 Katahira, Aoba-ku, Sendai 980-8577, Japan

²*Department of Electronic Engineering,*

Graduate School of Engineering, Tohoku University,

Aoba 6-6-05, Aramaki, Aoba-Ku, Sendai 980-8579, Japan

³*WPI Advanced Institute for Materials Research, Tohoku University,*

2-1-1 Katahira, Aoba-ku, Sendai 980-8577, Japan

⁴*ROHM Co., Ltd, 21 Saiinnmizosakicho,*

Ukyo-ku, Kyoto, Kyoto 615-8585, Japan

⁵*Center for Science and Innovation in Spintronics,*

Tohoku University, 2-1-1 Katahira, Aoba-ku, Sendai 980-8577, Japan

⁶*Center for Emergent Matter Science, RIKEN,*

2-1 Hirosawa, Wako, Saitama 351-0198, Japan

Abstract

GaN is expected to be a key material for next-generation electronics due to its interesting properties. However, the current collapse poses a challenge to the application of GaN FETs to electronic devices. In this study, we investigate the formation of quantum dots in GaN FETs under the current collapse. By comparing the Coulomb diamond between standard measurements and those under current collapse, we find that the gate capacitance is significantly decreased by the current collapse. This suggests that the current collapse changes the distribution of trapped electrons at the device surface, which is reported in the previous study by operando X-ray spectroscopy. Also, we show external control of quantum dot formation, previously challenging in an FET structure, by using current collapse.

Gallium nitride (GaN), a wide bandgap semiconductor featuring direct transitions, is renowned for forming high-mobility two-dimensional electron gases (2DEGs) at the GaN/AlGaN heterostructure interface [1–4]. This property positions GaN as a pivotal material for next-generation electronics, including power electronics and 5G technology applications. In the high power operation of GaN field-effect transistors (FETs), a challenge arises from a phenomenon known as current collapse [5, 6]. Current collapse induces an increase in on-resistance and fluctuations of the output current by applying high electric fields. This phenomenon critically hampers the device’s ability to perform as expected. It is suggested that the surface states of the device and the interface states between the gate insulator and AlGaN significantly contribute to this issue. Current collapse poses a key issue for the application of GaN FETs into electronic devices [5]. Its mechanism has been investigated through various methods, including transport measurements [7–12] and operando X-ray spectroscopy [13, 14]. To gain a more microscopic view, operando X-ray spectroscopy is a powerful technique for probing the electron state with high temporal and spatial resolution [15], which local information is difficult to access by the typical electron transport measurement. Thanks to various approaches, the mechanism of the current collapse is becoming increasingly clear.

From the perspective of quantum devices [16, 17], GaN is attractive because of its wide and direct bandgap. These characteristics can provide high-temperature operation and coupling with light [18]. Previously, quantum transport is observed in GaN devices with a gate voltage defined [19, 20], nano-structures [21–23], or a simple FET structures [24–26]. In particular, orbital excited states is also observed in the FET structure with fine gate electrode [25]. This result opens the fascinating application of the GaN quantum devices, such as a quantum bit operation. Quan-

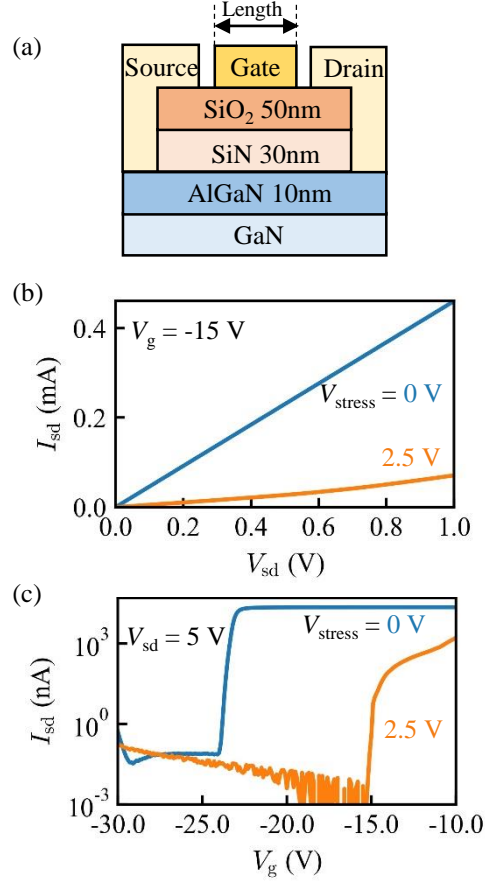


FIG. 1. (a) Schematic of the layer structure of the device. (b) I_{sd} - V_{sd} and (c) I_{sd} - V_g characteristics with and without the stress voltage at 2.3 K.

tum dots in the simple FET structure are formed by disordered potential fluctuation induced by impurities and defects [24, 25]. This mechanism suggests that surface electron trapping caused by the current collapse also affects the characteristics of the quantum dots. By utilizing this sensitivity, it is possible to probe the local distribution of surface electrons. In this study, we shed light on the microscopic perspective of the distribution of surface electrons by analyzing electron transport through GaN quantum dots under the current collapse.

Fig. 1(a) shows a layer structure of our device. GaN and AlGaN layers are deposited on the Si substrate by chemical vapor deposition. The 2DEG is formed at the interface between the GaN and AlGaN layers. The typical electron density and mobility of our layer structure are $6.7 \times 10^{12} \text{ cm}^{-2}$ and $1670 \text{ cm}^2\text{V}^{-1}\text{s}^{-1}$, respectively. The source and drain electrodes are constructed using Ti/Al metals. The devices are fabricated with gate lengths of 0.6, 0.8, and 1.4 μm . In order to induce the

current collapse, a stress voltage V_{stress} is applied to the source electrode in the pinch-off state at 300 K, which state is maintained for 1 hour. Subsequently, devices are cooled from 300 K to 2.3 K using a helium decompression refrigerator, spending approximately 2 hours keeping the V_{stress} .

After cooling, the source-drain current I_{sd} is measured as a function of the source-drain voltage V_{sd} , and a gate voltage V_{g} near the pinch-off state. The gate length of the measured device is 0.6 μm . Figure 1(b) shows the $I_{\text{sd}}-V_{\text{sd}}$ characteristics at 2.3 K. The blue line indicates the result without applying a stress voltage, while the orange line with $V_{\text{stress}} = 2.5$ V. During the measurement, V_{g} is set to the 'on' state at $V_{\text{g}} = -15$ V. When the stress voltage is applied, compared to the standard measurement, I_{sd} is significantly reduced, and an increase in the on-resistance is observed. The current collapse is caused by cooling the sample with the application of stress voltage. Figure 1(c) also shows the V_{g} dependence of I_{sd} at 2.3 K. The blue line represents the results from the standard measurement, while the orange line indicates the current collapse condition. Here, the V_{sd} is set to 5 V. The application of stress voltage results in a shift of the pinch-off voltage towards the positive side, which is approximately +10 V. The shift in pinch-off due to the thermal cooling from 300 K to 2.3 K is typically around 1.5 V in our devices. Therefore, this large change of shift voltage is due to electrons trapped at the AlGaIn/SiN interface and/or defect levels in the insulator.

Figure 2(a) shows the results of the FET characteristics near the pinch-off voltage for the device with a gate length of 0.6 μm , and the result measured under the current collapse condition ($V_{\text{stress}} = 2.5$ V) is also displayed in Fig 2(b). The differential conductance $dI_{\text{sd}}/dV_{\text{sd}}$ is plotted on a logarithmic scale against V_{sd} and V_{g} . In both cases, the $dI_{\text{sd}}/dV_{\text{sd}}$ is suppressed, displaying unique shapes as shown in the figures. These are Coulomb diamonds due to the formation of quantum dots in the conduction channel [24, 25]. The shape of the Coulomb diamond under the current collapse, especially in the V_{g} axis direction, is about five times larger than the standard measurement. Table I shows the electrostatic capacitances between the quantum dot and each electrode, the total electrostatic capacitance C , and the coefficient α that converts gate voltage to electrostatic energy called lever arm [27]. Each capacitance is determined from the shape of the Coulomb diamond by assuming the capacitive model [17, 28–30], as shown in Fig. 2(c). The electrostatic capacitance C_{g} between the quantum dot and the gate electrode significantly decreases under current collapse. α also decreases by two orders of magnitude, indicating a reduced contribution of the C_{g} to the total electrostatic capacitance C . Furthermore, C_{s} and C_{d} , the electrostatic capacitances between the quantum dot and the source and drain electrodes, are close in the standard measurement, while C_{s} is about three times larger than C_{d} under the current collapse.

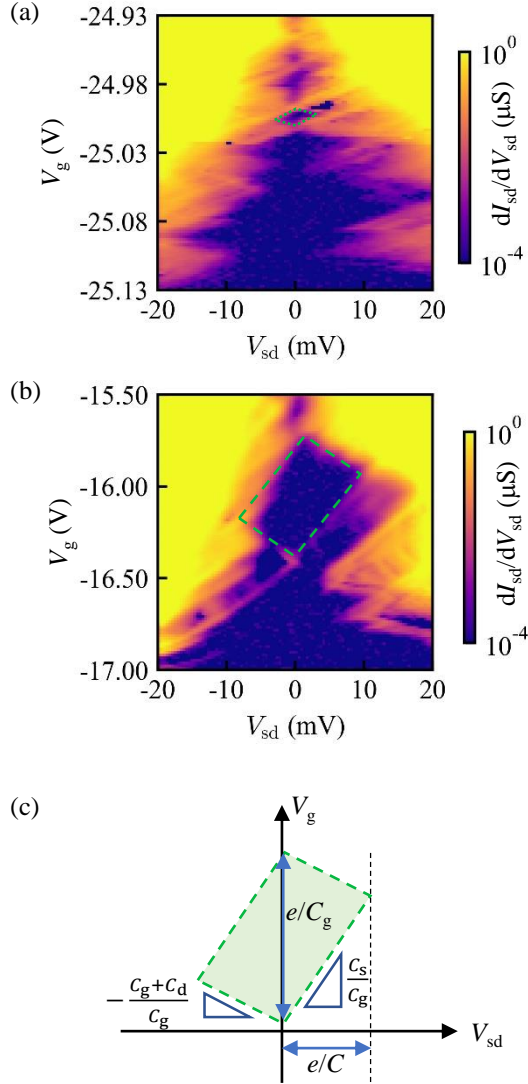


FIG. 2. (a) Color map of the dI_{sd}/dV_{sd} as a function of V_{sd} and I_g in a standard measurement and (b) under the current collapse. The dashed green area corresponds to the analyzed diamond. (c) Schematic of the Coulomb diamond.

TABLE I. Summary of electrostatic capacitances. Units of each capacitance are aF.

	C_g	C_s	C_d	C	$\alpha = C_g/C$
Standard	8.3	25.8	23.8	56.7	0.15
Collapse	0.2	10.3	3.3	13.8	0.0016

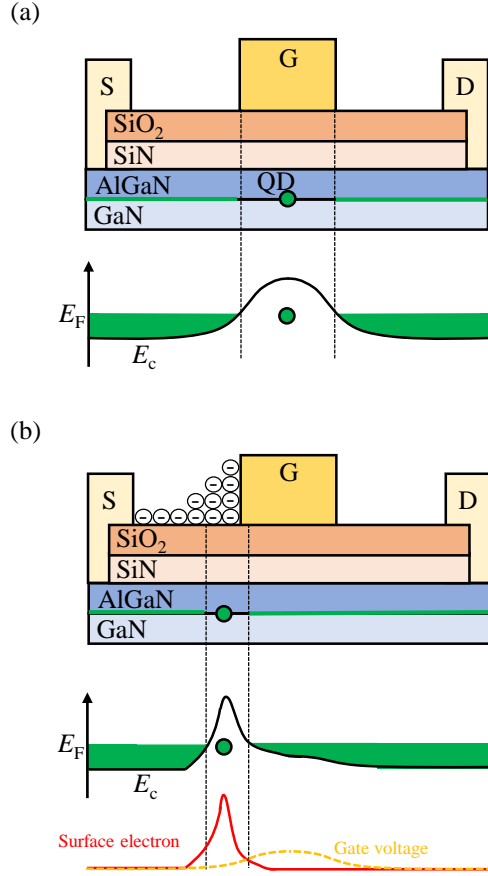


FIG. 3. Schematic of the surface electron trapping and an energy band structure (a) in the case of the standard measurement and (b) the current collapse.

The change in electrostatic capacitance can be qualitatively understood and is consistent with the insights of previous studies using operando X-ray spectroscopy [13, 14]. Near the pinch-off voltage under the standard measurement, the spatial profile of the conduction band's bottom energy level E_c is as shown in Fig. 3(a). The quantum dot is formed directly below the gate electrode and is almost symmetrically connected to both the source and drain electrodes. When the stress voltage is applied to the source electrode, electrons are trapped in surface levels towards the source from the gate electrode, as illustrated in Fig. 3(b). This electron trapping causes the change in the E_c profile. E_c rises steeply at the edge of the gate electrode and decreases gradually towards the source electrode. Therefore, near the pinch-off voltage under current collapse, it is expected that the formation of the quantum dot is not directly below the gate electrode but near the edge of the gate electrode where electron trapping occurs. Consequently, the coupling between the gate

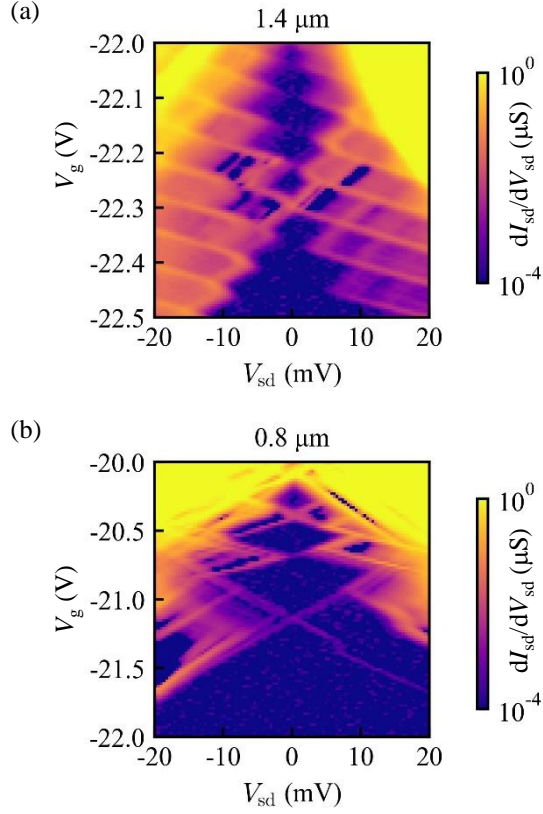


FIG. 4. The gate length dependence of the Coulomb diamond. Each length is (a) 1.4 and (b) 0.8 μm , respectively.

electrode and the quantum dot becomes smaller under current collapse, resulting in the decrease in C_g . Additionally, due to the superposition of the surface electron potential and the gate voltage set near the pinch-off region, an asymmetric coupling of the quantum dot and electrodes occurs, leading to the imbalance of C_d and C_s . These results can serve as a probing tool to investigate the distribution of surface electron trapping, which was previously challenging to access with simple transport measurements.

Finally, we measure the gate length dependence of the Coulomb diamond under the current collapse. The stress voltage is set to be 5 V in all devices. Clearly seen in Fig. 4, both devices show a completely closed Coulomb diamond. In the case of the standard condition, such a closed diamond is observed in the device with gate length below 0.2 μm [25]. This result suggests that the current collapse makes an effective short gate length structure in the vicinity of the gate electrode edge, as shown in Fig. 3(b). This built-in short gate forms a locally confined structure regardless

of the device's gate length, resulting in closed diamonds even in devices with longer gate lengths.

In this study, we investigate the formation of quantum dots under the current collapse in GaN FETs. The devices are cooled in their on state while applying a stress voltage. Under the current collapse, the width of the Coulomb diamond in the V_g axis direction increases compared to standard measurements. From the Coulomb diamond, we evaluate the electrostatic capacitance between quantum dots and each electrode, which can be explained by electron trapping by surface states. The gate length dependence of Coulomb diamond measurement shows that the current collapse can form an effective short gate length, which is the potential method for tuning the quantum dot formation that is difficult to control artifactually in a simple FET structure. Our findings suggest that the quantum dots in GaN FETs can serve as a probe to the current collapse, and external control of quantum dot formation in simple FETs is enabled by utilizing the current collapse, conversely.

ACKNOWLEDGEMENTS

We thank S. Yamaguchi, RIEC Fundamental Technology Center and the Laboratory for Nanoelectronics and Spintronics for writing and technical support. Part of this work is supported by Rohm Collaboration Project, MEXT Leading Initiative for Excellent Young Researchers, Grants-in-Aid for Scientific Research (21K18592, 23H01789, 23H04490), Iketani Science and Technology Foundation Research Grant, and FRiD Tohoku University.

AUTHOR DECLARATIONS

Conflict of Interest

The authors have no conflicts to disclose.

Author Contributions

Takaya Abe: Conceptualization (lead); Data Curation (lead); Formal Analysis (lead); Investigation (lead); Methodology (lead); Visualization (lead); Writing/Review & Editing (equal).
Motoya Shinozaki: Conceptualization (equal); Data Curation (equal); Formal Analysis (equal); Investigation (equal); Methodology (equal); Visualization (equal); Writing/Original Draft (lead);

Writing/Review & Editing (equal); **Kazuma Matsumura**: Investigation (equal); Methodology (equal); Resources (equal); Writing/Review & Editing (equal); **Takumi Aizawa**: Investigation (equal); Methodology (equal); Writing/Review & Editing (equal); **Takeshi Kumasaka**: Methodology (equal); Resources (equal); Writing/Review & Editing (equal); **Norikazu Ito**: Resources (equal); Writing/Review & Editing (equal); **Taketoshi Tanaka**: Resources (equal); Writing/Review & Editing (equal); **Ken Nakahara**: Resources (equal); Writing/Review & Editing (equal); **Tomohiro Otsuka**: Conceptualization (equal); Methodology (equal); Funding Acquisition (lead); Supervision (lead); Writing/Review & Editing (lead).

* motoya.shinozaki.c1@tohoku.ac.jp

† tomohiro.otsuka@tohoku.ac.jp

- [1] O. Ambacher, J. Smart, J. Shealy, N. Weimann, K. Chu, M. Murphy, W. Schaff, L. Eastman, R. Dimitrov, L. Wittmer, *et al.*, Two-dimensional electron gases induced by spontaneous and piezoelectric polarization charges in N- and Ga-face AlGaIn/GaN heterostructures, *J. Appl. Phys.* **85**, 3222 (1999).
- [2] M. Manfra, K. Baldwin, A. Sergent, K. West, R. Molnar, and J. Caissie, Electron mobility exceeding 160000 cm²/Vs in AlGaIn/GaN heterostructures grown by molecular-beam epitaxy, *Appl. Phys. Lett.* **85**, 5394 (2004).
- [3] N. Thillozen, S. Cabanas, N. Kaluza, V. Guzenko, H. Hardtdegen, and T. Schäpers, Weak antilocalization in gate-controlled Al_xGa_{1-x}N/GaN two-dimensional electron gases, *Phys. Rev. B* **73**, 241311 (2006).
- [4] A. Shchepetilnikov, D. Frolov, V. Solovyev, Y. A. Nefyodov, A. Großer, T. Mikolajick, S. Schmult, and I. Kukushkin, Electron spin resonance in a 2d system at a GaN/AlGaIn heterojunction, *Appl. Phys. Lett.* **113**, 052102 (2018).
- [5] E. A. Jones, F. F. Wang, and D. Costinett, Review of commercial GaN power devices and GaN-based converter design challenges, *IEEEJ.Emerg.Sel.Top.Power Electron.* **4**, 707 (2016).
- [6] S. C. Binari, P. Klein, and T. E. Kazior, Trapping effects in GaN and SiC microwave FETs, *Proc. IEEE* **90**, 1048 (2002).
- [7] D. Bisi, M. Meneghini, C. De Santi, A. Chini, M. Dammann, P. Brueckner, M. Mikulla, G. Meneghesso, and E. Zanoni, Deep-level characterization in GaN HEMTs-Part I: Advantages and limitations of drain current transient measurements, *IEEE Trans. Electron Devices* **60**, 3166 (2013).

- [8] Y. Tokuda, DLTS Studies of Defects in n-GaN, ECS Trans. **75**, 39 (2016).
- [9] W. Yang, J.-S. Yuan, B. Krishnan, and P. Shea, Characterization of deep and shallow traps in GaN HEMT using multi-frequency CV measurement and pulse-mode voltage stress, IEEE Trans. Device Mater. Reliab. **19**, 350 (2019).
- [10] W. Yang and J.-S. Yuan, Experimental investigation of buffer traps physical mechanisms on the gate charge of GaN-on-Si devices under various substrate biases, Appl. Phys. Lett. **116** (2020).
- [11] S. Pan, S. Feng, X. Li, X. Zheng, X. Lu, X. He, K. Bai, Y. Zhang, and L. Zhou, Identifying the properties of traps in GaN high-electron-mobility transistors via amplitude analysis based on the voltage-transient method, IEEE Trans. Electron Devices **68**, 5541 (2021).
- [12] S. Pan, S. Feng, X. Li, K. Bai, X. Lu, Y. Zhang, L. Zhou, E. Rui, Q. Jiao, and Y. Tian, Characterization of traps in GaN-based HEMTs by drain voltage transient and capacitance deep-level transient spectroscopy, Semicond. Sci. Technol. **37**, 095017 (2022).
- [13] K. Omika, Y. Tateno, T. Kouchi, T. Komatani, S. Yaegassi, K. Yui, K. Nakata, N. Nagamura, M. Kotsumi, K. Horiba, *et al.*, Operation mechanism of GaN-based transistors elucidated by element-specific x-ray nanospectroscopy, Sci. Rep. **8**, 13268 (2018).
- [14] K. Omika, K. Takahashi, A. Yasui, T. Ohkuchi, H. Osawa, T. Kouchi, Y. Tateno, M. Suemitsu, and H. Fukidome, Dynamics of surface electron trapping of a GaN-based transistors revealed by spatiotemporally resolved x-ray spectroscopy, Appl. Phys. Lett. **117** (2020).
- [15] H. Fukidome, K. Nagashio, N. Nagamura, K. Tashima, K. Funakubo, K. Horiba, M. Suemitsu, A. Toriumi, and M. Oshima, Pinpoint operando analysis of the electronic states of a graphene transistor using photoelectron nanospectroscopy, Appl. Phys. Express **7**, 065101 (2014).
- [16] S. Tarucha, D. G. Austing, T. Honda, R. J. van der Hage, and L. P. Kouwenhoven, Shell filling and spin effects in a few electron quantum dot, [Phys. Rev. Lett.](#) **77**, 3613 (1996).
- [17] L. P. Kouwenhoven, D. Austing, and S. Tarucha, Few-electron quantum dots, Rep. Prog. Phys. **64**, 701 (2001).
- [18] J. Luo, Y. Geng, F. Rana, and G. D. Fuchs, Room temperature optically detected magnetic resonance of single spins in GaN, Nat. Mater. **23**, 512 (2024).
- [19] H. Chou, S. Lüscher, D. Goldhaber-Gordon, M. Manfra, A. Sergent, K. West, and R. Molnar, High-quality quantum point contacts in GaN/ AlGaIn heterostructures, Appl. Phys. Lett. **86** (2005).
- [20] H. Chou, D. Goldhaber-Gordon, S. Schmult, M. Manfra, A. Sergent, and R. Molnar, Single-electron transistors in GaN/ AlGaIn heterostructures, Appl. Phys. Lett. **89** (2006).

- [21] J. Ristić, E. Calleja, A. Trampert, S. Fernández-Garrido, C. Rivera, U. Jahn, and K. H. Ploog, Columnar AlGa_N/Ga_N nanocavities with AlN/GaN bragg reflectors grown by molecular beam epitaxy on si (111), *Phys. Rev. Lett.* **94**, 146102 (2005).
- [22] T. Nakaoka, S. Kako, Y. Arakawa, and S. Tarucha, Coulomb blockade in a self-assembled Ga_N quantum dot, *Appl. Phys. Lett.* **90**, 162109 (2007).
- [23] R. Songmuang, G. Katsaros, E. Monroy, P. Spathis, C. Bougerol, M. Mongillo, and S. De Franceschi, Quantum Transport in Ga_N/AlN Double-Barrier Heterostructure Nanowires, *Nano Lett.* **10**, 3545 (2010).
- [24] T. Otsuka, T. Abe, T. Kitada, N. Ito, T. Tanaka, and K. Nakahara, Formation of quantum dots in Ga_N/AlGa_N FETs, *Sci. Rep.* **10**, 15421 (2020).
- [25] K. Matsumura, T. Abe, T. Kitada, T. Kumasaka, N. Ito, T. Tanaka, K. Nakahara, and T. Otsuka, Channel length dependence of the formation of quantum dots in Ga_N/AlGa_N FETs, *Appl. Phys. Express* **16**, 075003 (2023).
- [26] Y. Fujiwara, M. Shinozaki, K. Matsumura, K. Noro, R. Tataka, S. Sato, T. Kumasaka, and T. Otsuka, Wide dynamic range charge sensor operation by high-speed feedback control of radio-frequency reflectometry, *Appl. Phys. Lett.* **123** (2023).
- [27] K. Ono, T. Tanamoto, and T. Ohguro, Pseudosymmetric bias and correct estimation of Coulomb/confinement energy for unintentional quantum dot in channel of metal-oxide-semiconductor field-effect transistor, *Appl. Phys. Lett.* **103** (2013).
- [28] R. Nuryadi, H. Ikeda, Y. Ishikawa, and M. Tabe, Ambipolar Coulomb blockade characteristics in a two-dimensional Si multidot device, *IEEE Trans. Nanotechnol.* **2**, 231 (2003).
- [29] X.-X. Song, D. Liu, V. Mosallanejad, J. You, T.-Y. Han, D.-T. Chen, H.-O. Li, G. Cao, M. Xiao, G.-C. Guo, and G.-P. Guo, A gate defined quantum dot on the two-dimensional transition metal dichalcogenide semiconductor WSe₂, *Nanoscale* **7**, 16867 (2015).
- [30] Y. Muto, T. Nakaso, M. Shinozaki, T. Aizawa, T. Kitada, T. Nakajima, M. R. Delbecq, J. Yoneda, K. Takeda, A. Noiri, A. Ludwig, A. D. Wieck, S. Tarucha, A. Kanemura, M. Shiga, and T. Otsuka, Visual explanations of machine learning model estimating charge states in quantum dots, *APL Mach. Learn.* **2**, 026110 (2024).